Electronic Supplementary Information (ESI) for

High impact of the reducing agent on palladium nanomaterials: New insights from X-ray photoelectron spectroscopy and oxygen reduction reaction

Yaovi Holade,[a] Christine Canaff,[a] Suzie Poulin,[a] Têko W. Napporn,[a]* Karine Servat[a] and K. Boniface Kokoh[a]

*Corresponding author: teko.napporn@univ-poitiers.fr

1. Fundamentals of Oxygen Reduction Reaction in aqueous medium

1.1. General concepts

The oxygen reduction reaction (ORR) is effectively studied at an electrode material by some basic but fundamental relationships. Before starting any data analysis, it is important to understand these major gates. As emphasized by Jia and coworkers,[1] fundamental understanding of the ring rotation disc electrode (RRDE) theoretical basics and practical use is necessary to make appropriate use in an ORR study. The basic and current definitions and activity targets of ORR can be found in a review paper of Debe.[2] Depending of the medium, the ORR does not involve the same steps. Consequently, the whole reaction differs from the pH. In general, the overall reaction, which takes place in acidic medium, is described by Eq. (1) and involves the redox couple O_2/H_2O. Conversely, there is consumption of H_2O molecules in alkaline medium according to Eq. (2) and the involved redox couple is O_2/HO^-.

$$O_2 + 4H_3O^+ + 4e^- \rightleftharpoons 6H_2O \quad (1)$$

$$O_2 + 2H_2O + 4e^- \rightleftharpoons 4HO^- \quad (2)$$

The Nernst equation is used to determine the equilibrium potential. Remember that, in this case, the potential is scaled with the Standard Hydrogen Electrode (SHE) and is calculated as following by Eq. (3) in acidic medium and Eq. (4) in alkaline medium:

$$E_{O_2/H_2O}/(\text{V vs. SHE}) = E^0_{O_2/H_2O} + \frac{RT}{4F}\ln\left\{\frac{C_{O_2}}{C^0}\left(\frac{[H_3O^+]}{C^0}\right)^4\right\} \quad (3)$$

$$E_{O_2/H_2O}/(\text{V vs. SHE}) = E^0_{O_2/HO^-} + \frac{RT}{4F}\ln\left\{\frac{C_{O_2}}{C^0}\left(\frac{C^0}{[HO^-]}\right)^4\right\} \quad (4)$$

- C^0: reference molar concentration (= 10^{-3} mol cm^{-3}),
- R: gas constant (8.314 J K^{-1} mol^{-1}),
- T: temperature in Kelvin (T= 273.15+ θ, where θ is the temperature in °C),
- F: Faraday's constant (96 485 C mol^{-1}),
- C_{O2}: oxygen solubility (mol cm^{-3}),
- $[H_3O^+]$ is the H_3O^+ concentration (mol cm^{-3}),
- So, $E^0_{O_2/H_2O}$ = 1.229 V vs. SHE is the standard equilibrium potential of O_2/H_2O,
- So, $E^0_{O_2/HO^-}$ = 0.399 V vs. SHE is the standard equilibrium potential of O_2/HO^-.

Please note that, SHE is a virtual reference electrode. It cannot be fabricated experimentally because it involves standard conditions (1 bar, pH = 0) at 273.15 K.[3] So, during ORR experiments, many reference electrodes are currently used.[3-9] Depending on the electrolytic medium (which induces the pH value, and chemical species constant change), it is more convenient to convert these values *versus* the Reversible Hydrogen Electrode (RHE). In the case of SHE, the conversion of the potential into RHE (Reversible Hydrogen Electrode) is describe by Eq. (5) in acid medium.

$$E_{O_2/H_2O}/(\text{V vs. RHE}) = \left(E^0_{O_2/H_2O} + \frac{RT}{4F} \ln\left\{ \frac{C_{O_2}}{C^0} \left(\frac{[H_3O^+]}{C^0} \right)^4 \right\} \right) - \left(E^0_{H^+/H_2} + \frac{RT}{4F} \ln\left\{ \left(\frac{[H_3O^+]}{C^0} \right)^4 \right\} \right)$$

$$E_{O_2/H_2O}/(\text{V vs. RHE}) = E^0_{O_2/H_2O} + \frac{RT}{4F} \ln\left(\frac{C_{O_2}}{C^0} \right) \quad (5)$$

where $E^0_{O_2/H_2O} = 1.229 \text{ V vs. SHE}$ and $E^0_{H^+/H_2} = 0.000 \text{ V vs. SHE}$ at 25 °C.

From the water dissociation constant: $Ke = [HO^-] \times [H_3O^+]$ and

$$E_{O_2/H_2O}/(\text{V vs. RHE}) = \left(E^0_{O_2/HO^-} + \frac{RT}{4F} \ln\left\{ \frac{C_{O_2}}{C^0} \left(\frac{C^0}{[HO^-]} \right)^4 \right\} \right) - \left(E^0_{H^+/H_2} + \frac{RT}{4F} \ln\left\{ \left(\frac{[H_3O^+]}{C^0} \right)^4 \right\} \right)$$

the equilibrium potential must be evaluated according to Eq. (6) in alkaline medium.

$$E_{O_2/H_2O}/(\text{V vs. RHE}) = E^0_{O_2/HO^-} + \frac{RT}{4F} \ln\left(\frac{C_{O_2}}{Ke^4 C^0} \right) \quad (6)$$

where $E^0_{O_2/HO^-} = 0.399 \text{ V vs. SHE}$ at 25 °C.

All the important data involved in ORR results analysis are gathered in **Table S1**. It is obvious that any change of the experimental conditions induces a variation of the equilibrium potential (E_{eq}).

Table S1 Fundamental basic data of the ORR at 25-50 °C in different supporting electrolytes.

Electrolyte solution (25 °C, 1 atm)	**E_{eq}[a] (V *vs.* RHE)**	**D_{O2}[b] ($cm^2\ s^{-1}$)**	**υ[b] ($cm^2\ s^{-1}$)**	**C_{O2}[b] ($mol\ cm^{-3}$)**
0.5 M H_2SO_4 (Refs. [10-14])	1.184	2.01×10^{-5}	1.07×10^{-2}	1.03×10^{-6}
0.1 M $HClO_4$ (Refs. [10,12,15])	1.185	1.93×10^{-5}	1.01×10^{-2}	1.26×10^{-6}
0.1 M NaOH (Refs. [12,14])	1.183	1.90×10^{-5}	9.97×10^{-3}	8.35×10^{-7}
0.1 M KOH (Refs. [12,14])	1.185	1.90×10^{-5}	1.00×10^{-2}	1.2×10^{-6}
[a]These values are calculated from Nernst-based equations: Eq. (5) and Eq. (6). [b]These data are those from the indicated literature references in the first column.				

1.2. Data analysis through ORR equations

The ORR is described by Koutecky-Levich equation, Eq. (7).[11,14,16]

$$\frac{1}{j} = \frac{1}{j_l^{diff}} + \frac{1}{j_k^{app}} = \frac{1}{j_l^{diff}} + \left(\frac{1}{j_l^{film}} + \frac{1}{j_l^{ads}} + \frac{1}{j_0 \frac{\theta}{\theta_{eq}} e^{\frac{\eta}{b}}} \right) \tag{7}$$

with:

$$\frac{1}{j_L} = \frac{1}{j_l^{film}} + \frac{1}{j_l^{ads}}$$

$$\frac{1}{j_k} = \frac{1}{j_L} + \frac{1}{j_0 \frac{\theta}{\theta_{eq}} e^{\frac{\eta}{b}}}$$

$$j_k^{app} = j_0 \frac{\theta}{\theta_{eq}} e^{\frac{\eta}{b}}$$

$$\eta = E - E_{eq}$$

$$b = \frac{RT}{\alpha n F}$$

$$j_l^{diff} = 0.201 n F \upsilon^{-\frac{1}{6}} C_{O_2} D_{O_2}^{\frac{2}{3}} \Omega^{\frac{1}{2}} = nB\Omega^{\frac{1}{2}} \quad \text{where} \quad B = 0.201 F \upsilon^{-\frac{1}{6}} C_{O_2} D^{\frac{2}{3}} \tag{8}$$

- j: ORR current density ($mA \cdot cm^{-2}$),
- j_l^{diff} : diffusion limiting current density of O_2 in the bulk electrolyte ($mA\ cm^{-2}$),
- j_k: kinetic current density ($mA \cdot cm^{-2}$), free from the mass transport,

- j_l^{film} : diffusion limiting current density of O_2 inside the film composed of the catalytic ink ($mA \cdot cm^{-2}$),
- j_l^{ads} : diffusion limiting current density associated with the O_2 adsorption at catalyst active site ($mA \cdot cm^{-2}$),
- j_0: exchange current density ($mA \cdot cm^{-2}$),
- n: exchange number of electrons,
- b: Tafel slope (V),
- η (= $|E-E_{eq}|$, overpotential (V),
- D_{O_2} : diffusion coefficient of O_2 in solution ($cm^2 \cdot s^{-1}$),
- C_{O_2} : the bulk concentration of O_2 in the electrolyte (10^{-3} mol cm^{-3}),
- υ: kinematic viscosity of the electrolyte ($cm^2 \cdot s^{-1}$),
- F: Faraday's constant (F = 96485 $C \cdot mol^{-1}$),
- Ω: RRDE speed (*rpm*).

In the electrode potential region where ORR is kinetically controlled by O_2 diffusion, Eq. (8) indicates that plotting j_l^{diff} vs. $\sqrt{\Omega}$ gives linear line and is known as "Levich plot". In order to extract the data of interest from the ORR polarization curves using the RRDE, the following relationships are currently used, supposing $\theta \approx \theta_{eq}$ that represent the degree of coverage of the platinum surface by oxygen containing adsorbed species at potential E and at the equilibrium potential E_{eq}, respectively:

$$\frac{1}{j_k} = \frac{1}{j_L} + \frac{1}{j_0 e^{\frac{\eta}{b}}} \Rightarrow \eta = b \ln\left(\frac{j_L}{j_0} \times \frac{j_k}{j_L - j_k}\right) \tag{9}$$

$$\frac{\partial \eta}{\partial\left(\log\left(\frac{j_k}{j_L - j_k}\right)\right)} = -b' = -b \times \ln(10) \approx -2.3\frac{RT}{\alpha n F} \tag{10}$$

The curve $\eta = f\left(\log\left(\frac{j_k}{j_L - j_k}\right)\right)$, known as «Tafel plot» is a straight line characterized by a Tafel slop $\alpha_{Tafel} = -b' = \frac{\partial \eta}{\partial\left(\log\left(\frac{j_k}{j_L - j_k}\right)\right)}$ and the intercept $\beta_{Tafel} = -b' \log\left(\frac{j_0}{j_L}\right)$.

Thus, j_0 is calculated from Eq. (11).

$$j_0 = 10^{-\frac{\beta_{Tafel}}{b'}} j_L \tag{11}$$

In practice, it is more convenient to use "b' = 2.3×b" as Tafel plot (Eq. (9)) where α is the symmetric factor, currently taken equal to 0.5. It is expressed in mV dec^{-1}. And j_0 must be compared to those from literature.[10,11,17,18] Overriding data from the ORR using RRDE apparatus concern the determination of the water formation efficiency at the disc, $p(H_2O)$, in direct relationship with the amount of hydrogen peroxide (H_2O_2) as reaction intermediate. The method was firstly developed by Jakobs et *al.*[13] in 1985 and then revised by Vork and Barendrecht in 1990.[19] Basically, each RRDE is characterized by its collection efficiency, N ($0 < N < 1$). During the ORR, O_2 is reduced at the disc (current: $I_D < 0$) and the intermediate H_2O_2 is radially swept outward away from the disk electrode and toward the ring electrode where it is oxidized to O_2 ring (current: $I_R > 0$). The set relationship is given by Eq. (12).[19] We draw reader's attention that even if N is provided in percentage, *e.g.* 20.5 % (herein), its value used in Eq. (12) is the fraction meaning 0.205. In alkaline medium, the intermediate is HO_2^-.

$$p(H_2O) = 1 - p(H_2O_2) = \frac{NI_D + I_R}{NI_D - I_R} = \frac{1 - \frac{I_R}{N|I_D|}}{1 + \frac{I_R}{N|I_D|}} \tag{12}$$

The O_2 reduction to H_2O or HO^- involves $4e^-$ and only $2e^-$ when the reaction process leads to H_2O_2 or HO_2^-. Thus, when both H_2O and H_2O_2 are produced (acid medium), the number of electrons exchanged during the oxygen reduction, n_{ex}, is easily accessed through Eq. (13).[13,19]

$$n_{ex} = n_{(O_2 \to H_2O)} + n_{(O_2 \to H_2O_2)} = 4p(H_2O) + 2p(H_2O_2) = 2\left[p(H_2O) + 1\right] = \frac{4N|I_D|}{N|I_D| + I_R} = \frac{4}{1 + \frac{I_R}{N|I_D|}} \leq 4 \tag{13}$$

As aforementioned, the collection efficiency is specific of the RRDE geometry and does not depend on the studied redox reaction.[14,16,20] It can also be experimentally measured using a simple reaction such as $[Fe(CN)_6]^{3-} + e^- \rightarrow [Fe(CN)_6]^{4-}$. It is calculated from Eq. (14)

$$N = -\frac{I_R}{I_D} = \frac{I_R}{|I_D|} \leq 1 \tag{14}$$

2. Additional Figures: Cyclic voltammetry

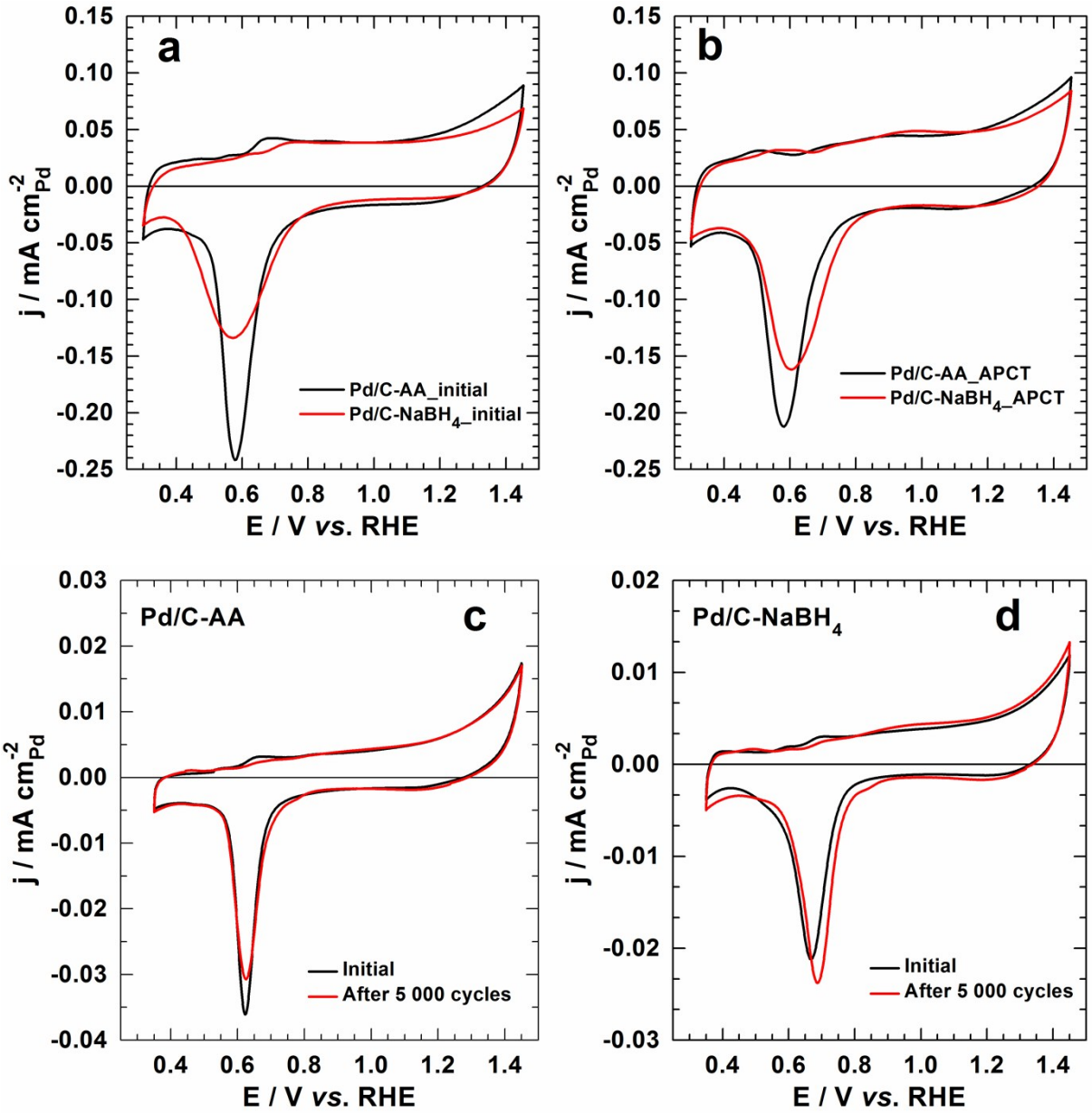

Fig. S1 Cyclic voltammograms recorded in N_2-saturated 0.1 mol L^{-1} KOH at 50 mV s^{-1} **(a, b)** and 50 mV s^{-1} **(c, d)** scan rates on Pd/C-AA and Pd/C-$NaBH_4$ electrode materials before and after the 5000 cycles of the accelerated potential cycling test (APCT) from 0.6 to 1 V vs. RHE at 100 mV s^{-1} scan rate in O_2-saturated 0.1 mol L^{-1} KOH. APCT was performed by cycling the disc electrode potential from 0.6 to 1 V vs. RHE at 100 mV s^{-1} scan rate in O_2-saturated 0.1 mol L^{-1} KOH solution.

3. Additional Figures: ORR experiments RRDE

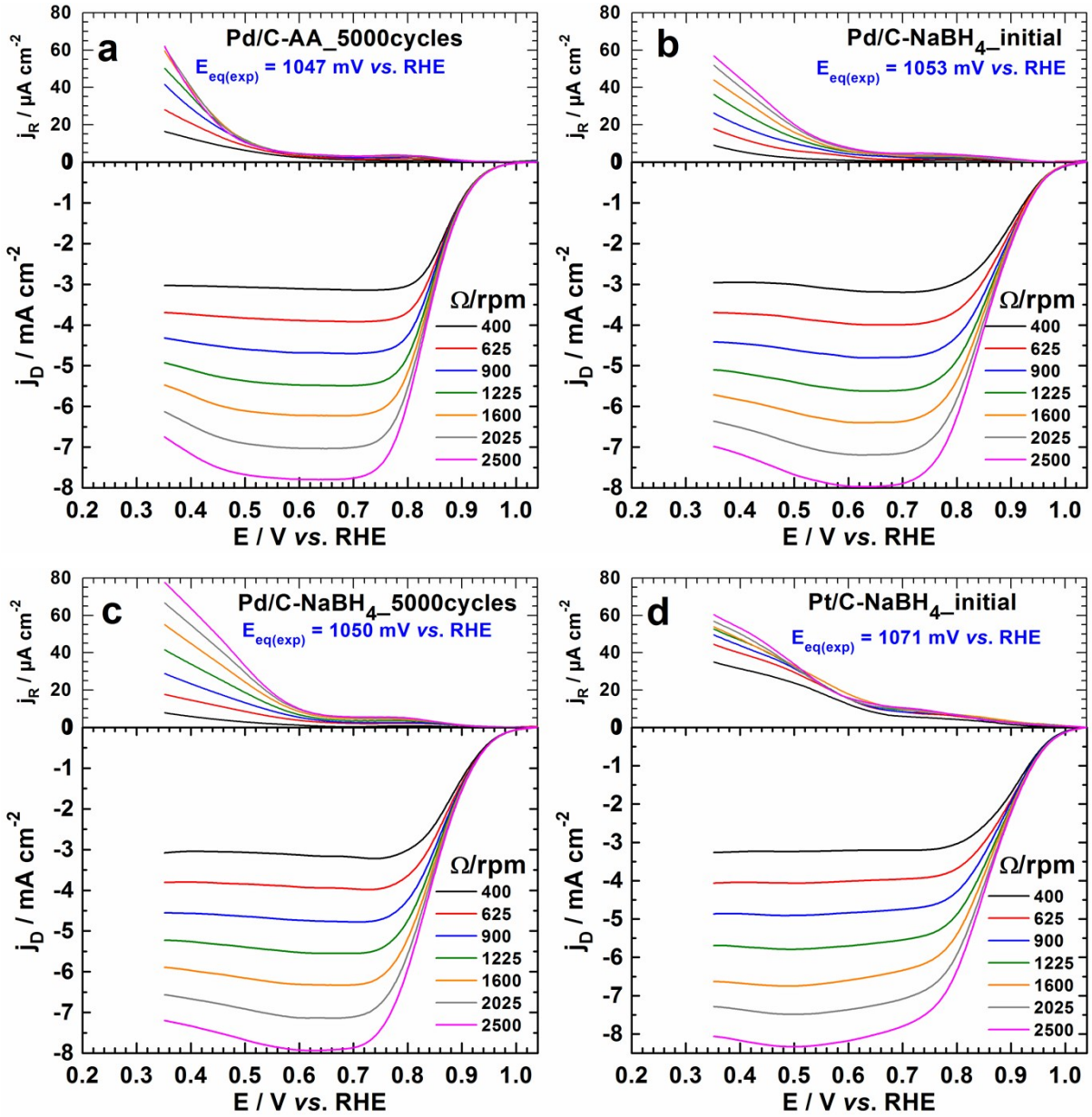

Fig. S2 ORR polarization curves recorded in O_2-saturated 0.1 mol L^{-1} KOH solution at the ring (top) and disc (bottom) for 5 mV s^{-1} scan rate for different speeds of the RRDE. **(a)** Pd/C-AA electrode material after 5000 cycles of the accelerated potential cycling test (APCT). Pd/C-$NaBH_4$ electrode material before **(b)** and after 5000 cycles of APCT **(c)**. **(d)** Pt/C electrode material before 5000 cycles of APCT. For all panels, the current densities are obtained with the geometry surface area of the ring (0.11 cm^2) and disc (0.196 cm^2). APCT was performed by cycling the disc electrode potential from 0.6 to 1 V vs. RHE at 100 mV s^{-1} scan rate in O_2-saturated 0.1 mol L^{-1} KOH solution.

4. Additional Figures: The Koutecky–Levich plots

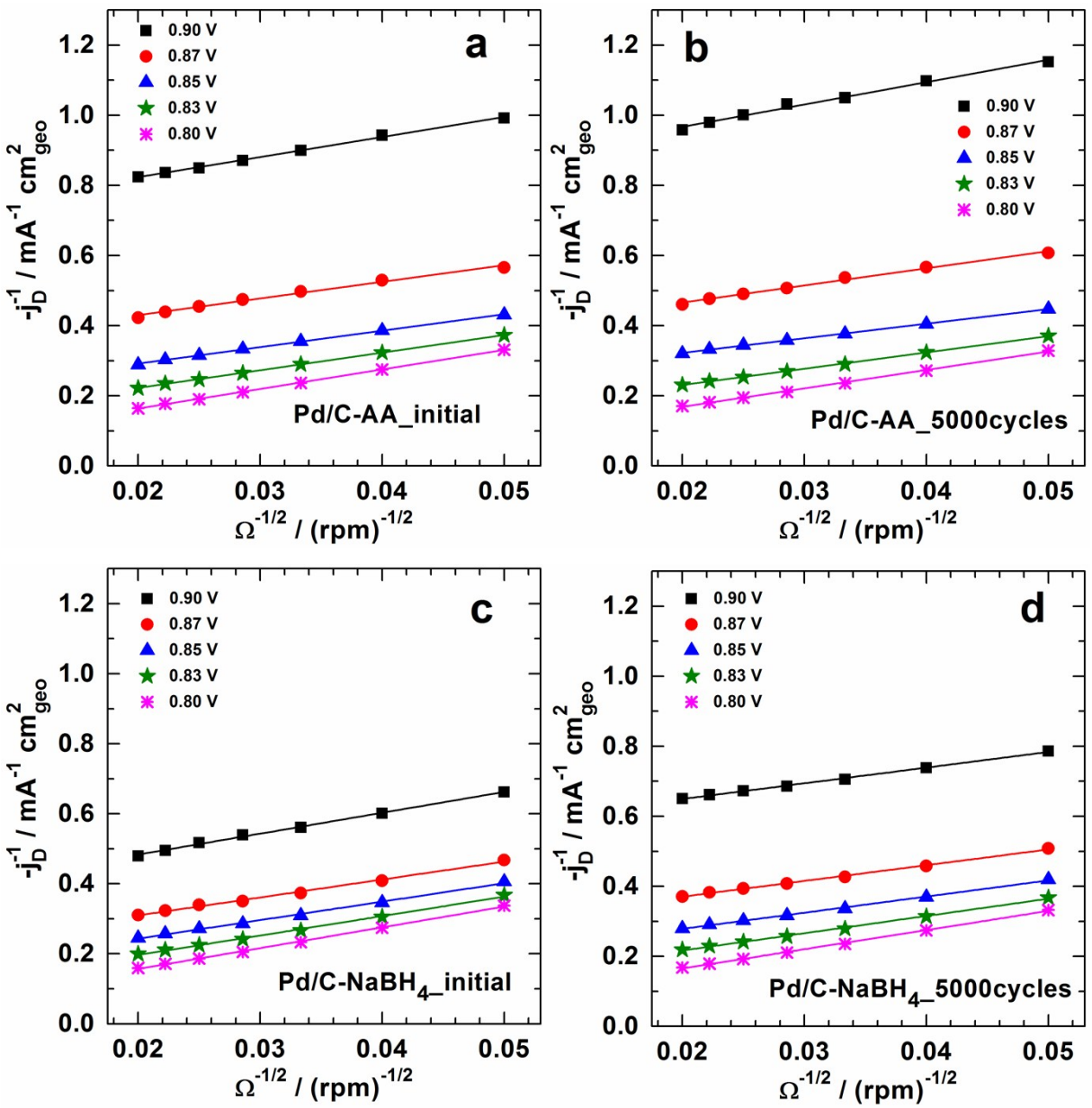

Fig. S3 The Koutecky–Levich plots from the ORR polarization curves recorded at 5 mV s^{-1} scan rate; before **(a, c)** and after **(b, d)** the 5000 cycles of accelerated potential cycling test (APCT). For all panels, the current densities are obtained with the geometry surface area of the ring (0.11 cm^2) and disc (0.196 cm^2). APCT was performed by cycling the disc electrode potential from 0.6 to 1 V vs. RHE at 100 mV s^{-1} scan rate in O_2-saturated 0.1 mol L^{-1} KOH solution.

5. Additional Figures: Determination of the limiting current density j_L

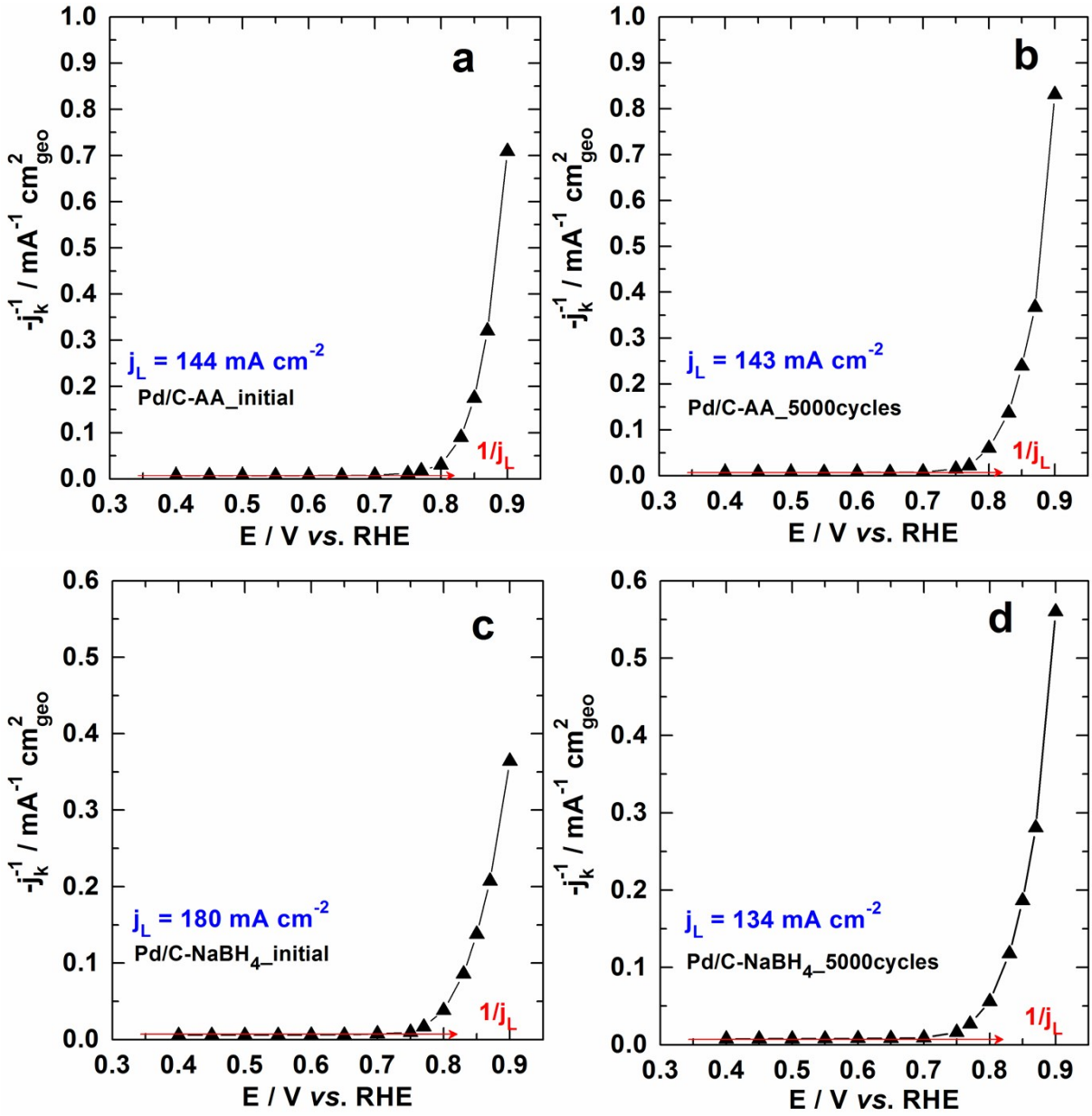

Fig. S4 The "j_k^{-1} *versus* E" plots for the determination of the limiting current density j_L before **(a, c)** and after **(b, d)** the 5000 cycles of accelerated potential cycling test (APCT). The obtained value is reported in each panel. Note: j_k is the kinetic current density, determined from the Koutecky–Levich plots and normalized with the geometry surface area of the disc (0.196 cm^2). APCT was performed by cycling the disc electrode potential from 0.6 to 1 V vs. RHE at 100 mV s^{-1} scan rate in O_2-saturated 0.1 mol L^{-1} KOH solution.

References:

1. Z. Jia, G. Yin and J. Zhang, in *Rotating Electrode Methods and Oxygen Reduction Electrocatalysts*, eds. W. Xing, G. Yin and J. Zhang, Elsevier, Amsterdam, 2014, pp. 199-229.
2. M. K. Debe, *Nature*, 2012, **486**, 43-51.
3. T. Biegler and R. Woods, *J. Chem. Educ.*, 1973, **50**, 604-605.
4. R. Thacker, *J. Chem. Educ.*, 1968, **45**, 180.
5. R. Thacker, *Nature*, 1963, **198**, 179-179.
6. W. J. Hamer and D. N. Craig, *J. Electrochem. Soc.*, 1957, **104**, 206-211.
7. T. J. Gray and R. Eiss, *Nature*, 1962, **194**, 469-470.
8. J. Engelhardt, *J. Chem. Educ.*, 1968, **45**, 547.
9. R. D. Caton, *J. Chem. Educ.*, 1973, **50**, A571-A578.
10. C. Song and J. Zhang, in *PEM Fuel Cell Electrocatalysts and Catalyst Layers*, ed. J. Zhang, Springer-Verlag London, London, UK, 2008, pp. 89-134.
11. C. Coutanceau, M. J. Croissant, T. Napporn and C. Lamy, *Electrochim. Acta*, 2000, **46**, 579-588.
12. K. E. Gubbins and R. D. Walker, *J. Electrochem. Soc.*, 1965, **112**, 469-471.
13. R. C. M. Jakobs, L. J. J. Janssen and E. Barendrecht, *Electrochim. Acta*, 1985, **30**, 1085-1091.
14. W. Xing, G. Yin and J. Zhang, *Rotating Electrode Methods and Oxygen Reduction Electrocatalysts*, Elsevier Science and Technology, Poland, 2014.
15. D. Wang, H. L. Xin, R. Hovden, H. Wang, Y. Yu, D. A. Muller, F. J. DiSalvo and H. D. Abruña, *Nat. Mater.*, 2013, **12**, 81-87.
16. Allen J. Bard and L. R. Faulkner, *Electrochemical Methods: Fundamentals and Applications*, John Wiley & Son, Inc., USA, 2001.
17. J. X. Wang, N. M. Markovic and R. R. Adzic, *J. Phys. Chem. B*, 2004, **108**, 4127-4133.
18. C. Song, Y. Tang, J. L. Zhang, J. Zhang, H. Wang, J. Shen, S. McDermid, J. Li and P. Kozak, *Electrochim. Acta*, 2007, **52**, 2552-2561.
19. F. T. A. Vork and E. Barendrecht, *Electrochim. Acta*, 1990, **35**, 135-139.
20. Y. V. Pleskov and V. Y. Filinovskii, *The Rotating Disc Electrode*, Consultants Bureau, New York, USA, 1976.